Regulating drift-wave plasma turbulence into spatiotemporal patterns by pinning coupling

Panpan Liu,[1] Lei Yang,[1] Zhigang Deng,[1] and Xingang Wang[1,2,*]
[1]*Institute for Fusion Theory and Simulation, Zhejiang University, Hangzhou, China 310027*
[2]*Department of Physics, Zhejiang University, Hangzhou, China 310027*
(Received 7 May 2011; published 11 July 2011)

Using the technique of pinning coupling in chaos control, we investigate how the two-dimensional drift-wave plasma turbulence described by the Hasegawa-Mima equation can be regulated into different spatiotemporal patterns. It is shown both analytically and numerically that, depending on the pattern structure of the target, the pinning strength necessary for regulating the turbulence could have a large variation. More specifically, with the increase of the wave number of the target, the critical pinning strength is found to be increased by a power-law scaling. Moreover, in both the transition and transient process of the pinning regulation, the modes of the turbulence are found to be suppressed in a *hierarchical* fashion, that is, by the sequence of mode wave number. The findings give insight into the dynamics of drift-wave turbulence, as well as indicative to the design of new control techniques for real-world turbulence.

DOI: 10.1103/PhysRevE.84.016207 PACS number(s): 05.45.Gg, 05.45.Xt

Over the past decade there have been continuous efforts in extending the concepts and techniques developed in the control of low-dimensional chaotic systems to high-dimensional distributed systems [1–3]. Owing to the spatial extent, the dynamics of high dimensional are much more complicated than the low-dimensional cases and, to tame it, the control techniques should be carefully selected or specially designed. A technique originated from chaos control and now being widely adopted in controlling high-dimensional systems is the method of pinning coupling, in which the system dynamics is "pulled" to a target by adding feedback signals to all or partial of the system variables [4–8]. Compared to other control techniques of distributed systems such as time-delay feedback and external forcing, the pinning technique has the distinct advantage of being able to regulate the system into various spatiotemporal patterns. The efficiency of pinning coupling has been manifested in a variety of high-dimensional distributed systems, including ensembles of coupled nonlinear oscillators [4,9], spatiotemporal chaos described by various partial differential equations [6,10], defect turbulence in cardiac system [11], and flow turbulence governed by the Novier-Stokes equations [12,13]. In these studies the target is often selected as one of the unstable solutions of the system, and an important task is to find the critical pinning strength that makes the solution stable.

Plasma system has been extensively studied in nonlinear science for either the purpose of dynamics exploration or as a test platform for the new techniques [1]. In the control of plasma systems, the previous studies have shown, both theoretically and experimentally, that in the chaotic regime (few unstable dimensions) the system dynamics is relatively easy to tame, while in the turbulence regime (a large number of unstable dimensions coexist), the control is much more difficult and challenging, for example, the control of drift-wave turbulence [14–19]. Drift-wave turbulence arises naturally in plasma columns where there exists a pressure gradient, and is generally believed to be responsible for the anomalous cross-field particle transport in magnetically confined high-temperature plasmas, such as in the tokamaks [20]. An interesting phenomenon discovered recently in high-temperature plasma is that drift-wave turbulence can sometimes self-organize into patterns of regular spatial structures, for example, the zonal flows, with which the anomalous transport can be significantly reduced [21]. However, in most of the practical situations, these spatial patterns are unstable and cannot be achieved by the system dynamics itself. Therefore, to induce them from the turbulence background, it is necessary to apply some control techniques. Using the technique of time-delay autosynchronization (TDAS) [22], it has been shown experientially that the chaotic temporal behavior of the drift-wave turbulence in a cylindrical magnetized plasma can be tamed to be periodic [15]. In another experiment, it has been shown that using the strategy of open-loop synchronization, namely the mode-selective control, the complicated spatial behavior of the drift-wave turbulence can also be tamed to a predefined pattern of regular spatial structure [17]. In theoretical studies, it has been shown recently that in one-dimensional (1D) linear plasma systems, both the spatial and temporal behaviors of the drift-wave turbulence can be tamed by using the strategy of pinning coupling [18].

In the present paper, using the method of pinning coupling, we will investigate how the drift-wave plasma turbulence as described by the two-dimensional (2D) Hasegawa-Mima equation can be regulated into spatially periodic and timely varying patterns. We would like to note that, besides the difference in the models (the 2D turbulence possesses many features that are absent in its 1D counterpart, e.g., the vortex structure, and is an important step toward the three-dimensional case of realistic systems), the questions to be addressed in the present work are also different from the previous studies of turbulence suppression. Specifically, the present work is focusing on *the influences of the target on the controllability of the drift-wave turbulence, and also the transition and transient process of the regulation*. These aspects are of important practical concerns to the implementation of the pinning strategy in realistic systems, but have not been well addressed in previous studies.

*wangxg@zju.edu.cn

The drift-wave plasma turbulence to be investigated is described by the following 2D Hasegawa-Mima equation [23]:

$$\partial_t(1-\nabla_\perp^2)\phi + V_d\partial_y(\phi) + [\nabla_\perp^2\phi,\phi] = 0, \quad (1)$$

with $\phi = \phi(x,y,t)$ the electrostatic potential, $[f,g] = \partial_y f\partial_x g - \partial_x f\partial_y g$ the Poisson bracket, and $\nabla_\perp^2 = \nabla_x^2 + \nabla_y^2$ the Laplace operator perpendicular to the magnetic field $\mathbf{B} = B\mathbf{e}_z$. Standard operations have been adopted to make the equation dimensionless, and the only tunable parameter of the equation is V_d, which characterizes the speed of the diamagnetic drift. The nonlinearity of the equation lies in the term $[\nabla_\perp^2\phi,\phi]$, which is caused by the nonlinear polarization drift. Throughout the study we will fix $V_d = 1$, with which the system is in the turbulence regime [24].

In the numerical simulations we set the system to be bounded in the square domain $[0,8\pi] \times [0,8\pi]$, and adopting the periodic boundary condition for each direction. The time increment Δt is chosen as 1×10^{-2} [in obtaining Eq. (1), the time t has been normalized by the ion gyroperiod], and the space is divided into 512×512 grids. The initial conditions are given in the Fourier space, which, for the sake of simplicity, are chosen as a combination of three plane waves, $\phi = \sum_{i=1}^{3} A_0 \cos(\mathbf{k}_i \cdot \mathbf{r})$, with $A_0 = 1 \times 10^{-2}$ and $\mathbf{k}_1 = (1,2), \mathbf{k}_2 = (1,3), \mathbf{k}_3 = (-3,-5)$. To integrate the equation, we adopt the Fourier pseudospectral method and the Adams-Bashforth-Crank-Nicolson (ABCN) scheme for the space and time discretizations, respectively [25]. The numerical results are verified by using different initial conditions, grids, and time increments. The equation is integrated for a period of length $t = 1 \times 10^3$, during which the system shows the typical behavior of 2D drift-wave turbulence, for example, the formation, interaction, and evolution of vortices. The system state ϕ at $t = 1 \times 10^3$ is shown in Fig. 1(a), which shall be taken as the reference turbulence state for the investigation of the pinning coupling in the present work.

With the pinning coupling, the equation of the system becomes

$$\partial_t(1-\nabla_\perp^2)\phi + V_d\partial_y(\phi) + [\nabla_\perp^2\phi,\phi] = \varepsilon(\phi - \phi_T), \quad (2)$$

with ϕ_T the spatiotemporal pattern, that is, the target, that the turbulence is going to be controlled to, and ε the strength of the pinning coupling. For simplicity, we choose the targets as the unstable analytical solutions of the Hasegawa-Mima equation $\phi_T = A_T \cos(\mathbf{k}_T \cdot \mathbf{r} - \omega_T t)$, with $\mathbf{k}_T = (k_T, k_T)$ and $\omega_T = k_T/(1+k_T^2)$. As a test of the pinning method, we set $A_T = 5 \times 10^{-2}$ and $\mathbf{k}_T = (1.25, 1.25)$ for the target, and using a relatively strong pinning strength, $\varepsilon = 0.2$ to regulate the turbulence in Fig. 1(a). As shown in Fig. 1(b), after $t = 1 \times 10^3$ of the pinning, the turbulence is well regulated to the target pattern.

The critical pinning strength ε_c necessary for regulating the turbulence can be theoretically analyzed in terms of the mode-mode interactions. Linearizing Eq. (2) around the target, we obtain the following equation for the perturbation:

$$\partial_t(1-\nabla_\perp^2)\delta\phi + V_d\partial_y(\delta\phi) + [\nabla_\perp^2\delta\phi,\phi_T] + [\nabla_\perp^2\phi_T,\delta\phi] = \varepsilon\delta\phi, \quad (3)$$

where $\delta\phi = \phi - \phi_T$. Rewriting $\phi_T = [A_T \exp(i\mathbf{k}_T \cdot \mathbf{r} - i\omega_T t + \varphi_T) + c.c]/2$ and $\delta\phi = \sum_i \delta\phi_i = \sum_i [\delta A_i(t)$

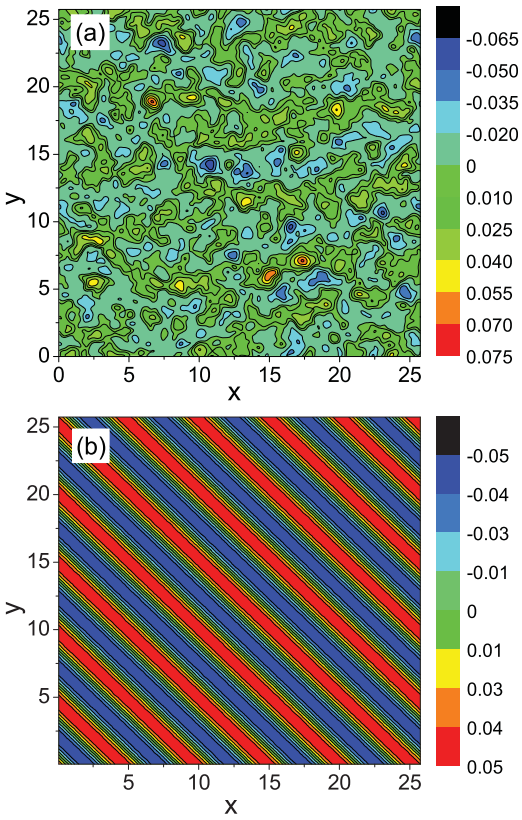

FIG. 1. (Color online) (a) The equipotential contours of ϕ for the 2D drift-wave turbulence generated by the Hasegawa-Mima equation. (b) For $\varepsilon = 0.2$, the equipotential contours of ϕ at $t = 1 \times 10^{-3}$ after the start of the pinning. It is seen that the drift-wave turbulence is successfully regulated to the target state with $\mathbf{k}_T = (1.25, 1.25)$.

$\exp(i\mathbf{k}_i \cdot \mathbf{r} - i\omega_i t + \varphi_i) + c.c]/2$, we are then able to transfer Eq. (3) into the Fourier space, and obtain a set of nonlinear coupled-mode equations. Considering only a pair of coupled modes (by the scheme of three-wave coupling, and regarding ϕ_T as the pumping wave), $\delta\phi_1$ and $\delta\phi_2$, from the set, their amplitudes are governed by equations

$$d\delta A_1/dt = C_{1,2}A_T^*\delta A_2^* e^{i\Delta\omega_{1,2}t} - \varepsilon_1\delta A_1, \quad (4)$$

$$d\delta A_2/dt = C_{2,1}A_T^*\delta A_1^* e^{i\Delta\omega_{1,2}t} - \varepsilon_2\delta A_2. \quad (5)$$

where $\varepsilon_i = \varepsilon/(1+k_i^2)$ and $C_{i,j} = (k_j^2 - k_T^2)(\mathbf{k_T} \times \mathbf{k}_j) \cdot \mathbf{e}_z/(1+k_i^2)$ is the coupling coefficient. $\Delta\omega_{1,2} = \omega_1 + \omega_2 + \omega_T$ is the frequency shift, which, due to the resonant condition $\mathbf{k}_1 + \mathbf{k}_2 + \mathbf{k}_T = 0$, is small and can be treated as 0. Please note that in deriving Eqs. (4) and (5) we have also employed the phase-match condition $\phi_1 + \phi_2 + \phi_T = 0$, which makes a selection on the coupled modes. The growth rates λ of the pair of coupled modes are then given by

$$\lambda^2 + (\varepsilon_1 + \varepsilon_2)\lambda + \left(\varepsilon_1\varepsilon_2 - C_{1,2}C_{2,1}A_T^2\right) = 0. \quad (6)$$

To keep the modes stable we must have $\lambda < 0$, which requires

$$\varepsilon > \varepsilon_c'(\mathbf{k}_1,\mathbf{k}_2,\mathbf{k}_T) = A_T\sqrt{(1+k_1^2)(1+k_2^2)C_{1,2}C_{2,1}}. \quad (7)$$

The above equation gives the necessary pinning strength for stabilizing a single pair of coupled modes in the perturbation.

To suppress the turbulence globally, all the perturbation modes should be stabilized. This means that the critical pinning strength is determined by the most-unstable mode (the mode that has the highest growth rate) of the system, that is, $\varepsilon_c = \varepsilon'_{\max} = \max\{\varepsilon'(\mathbf{k}_1,\mathbf{k}_2,\mathbf{k}_T)\}$. Because $\mathbf{k}_1 = -\mathbf{k}_2 - \mathbf{k}_T$, the critical pinning strength thus is determined by only two vectors $\varepsilon' = \varepsilon'(\mathbf{k},\mathbf{k}_T)$. For the given target pattern, that is, fixing the value of $\mathbf{k}_T$, the most-unstable mode $\mathbf{k}^{\max}$ can be determined by requiring $\partial\varepsilon'/\partial k_x = 0$ and $\partial\varepsilon'/\partial k_y = 0$, which give $k_x^{\max} \approx -2.1k_T$ and $k_y^{\max} = -0.66k_T$, respectively. Inserting these values into Eq. (7), we finally have

$$\varepsilon_c \approx A_T k_T^4. \tag{8}$$

The above equation is the main result of our work, which characterizes the influence of the target structure on the turbulence controllability.

Equation (8) shows that, as the pattern structure becomes complicated (increasing the value of k_T), it is more difficult to regulate the turbulence. While this phenomenon has been partially observed in previous studies of pinning control [13], to the best of our knowledge, it is the first time that the relationship between the turbulence controllability and the target structure is explicitly given. From the practical point of view, a quantitative estimate of the critical pinning strength could be beneficial to the control of realistic systems in many aspects. Taking the suppression of anomalous transport induced by plasma turbulence as an example, while it is desirable to regulate the turbulence into patterns of tiny structures (large wave numbers), the high cost of the larger pinning strength makes it difficult to be implemented in practice. Now, with Eq. (8), we might able to find a good balance between the performance and the cost of the pinning strategy.

The above analysis is well verified by numerical simulations. Adopting different patterns as the target, we plot in Fig. 2(a) the transition of the system dynamics as a function of the pinning strength. The degree of the regulation is characterized by the error $\delta = \sqrt{\sum_{i,j}^{N}(\phi_{i,j}-\phi_T)^2/N}$, with $N = 512$ the size of the simulation grid. The value of δ is evaluated at the moment $t = 1 \times 10^3$ after the start of the pinning, and the turbulence state is regarded as being successfully regulated if $\delta/A_T < 1 \times 10^{-3}$, where A_T is the amplitude of the target. From Fig. 2(a) it is seen clearly that, as the wave number of the target k_T increases, the critical pinning strength is gradually shifted to the larger values. The dependence of the controllability on the target wave number is more evident in Fig. 2(b), where the critical pinning strength ε_c is plotted as a function of the target wave number $\mathbf{k}_T$ in a wide range. As shown in Fig. 2(b), the numerical results fit the theoretical prediction of Eq. (8) very well.

In realistic situations, instead of being completely removed, sometimes the turbulence is only required to be suppressed below a certain level [21]. That is, a partial suppression of the turbulence. Also, from the practical point of view, it is favorable if the level of turbulence can be significantly (not fully) reduced by a lower control cost, say, for instance, by a small pinning strength in our case. Regarding this, it is necessary to have a study on the intermediate states of the system in the regime $\varepsilon \in (0,\varepsilon_c)$, that is, the transition of the

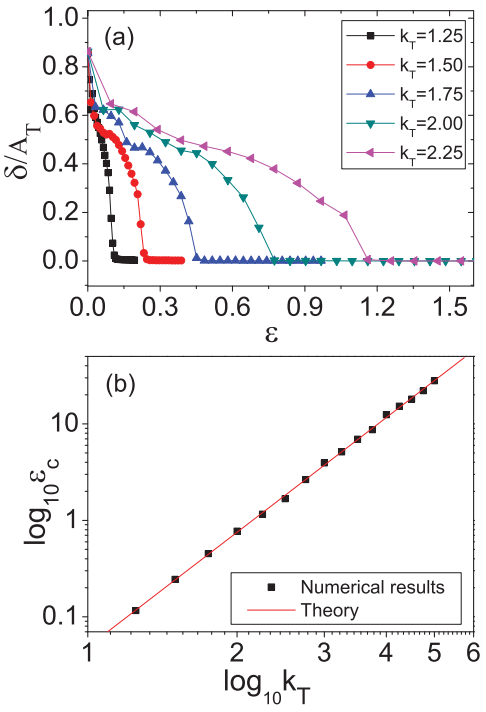

FIG. 2. (Color online) (a) Using different spatial patterns as the target, the variation of the normalized pinning error δ/A_T as a function of the pinning strength ε. (b) The variation of the critical pinning strength ε_c as a function of the wave number k_T. It is seen that the numerical results (the black squares) are well fitted by the theoretical result of Eq. (8) (the red line).

pinning regulation. The transition process can be understood by analyzing the theoretical result of Eq. (7). From Eq. (7) it is not difficult to find that in the space constructed by k_x and k_y, the value of ε'_c is symmetric about the line $k_x = k_y$ and, close to the origin, the value of ε'_c is monotonically increased with k_x and k_y. This gives an important indication to the property of the pinning transition: *the perturbation modes are suppressed by the sequence of wave number*. More specifically, as ε increases from 0, in the Fourier space it is expected to see a hierarchical suppression of the modes, starting from the central area (long-wave modes) and then propagating to the peripheral region (short-wave modes). This is indeed what observed in numerical simulations. For the same target as used in Fig. 1(b), we plot in Fig. 3 (the left column) several of the typical states appearing in the transition, where the hierarchical suppression of the perturbation modes is clearly shown. (We note that in Fig. 3 the sparse white points appearing in the boundary regions are due to the small amplitudes of the short-wave modes in the original turbulence state, which has nothing to do with the pinning coupling.)

The critical pinning strength characterizes only the long-time behavior of the system, but gives no information on the transient dynamics [26], for example, the time needed to pinning the turbulence. In many realistic situations, it is required that the turbulence should be regulated within a short period, say, for example, the turbulence suppression in the tokamaks. Regarding this, it is necessary to investigate the transient dynamics of the pinned system. Specifically, for

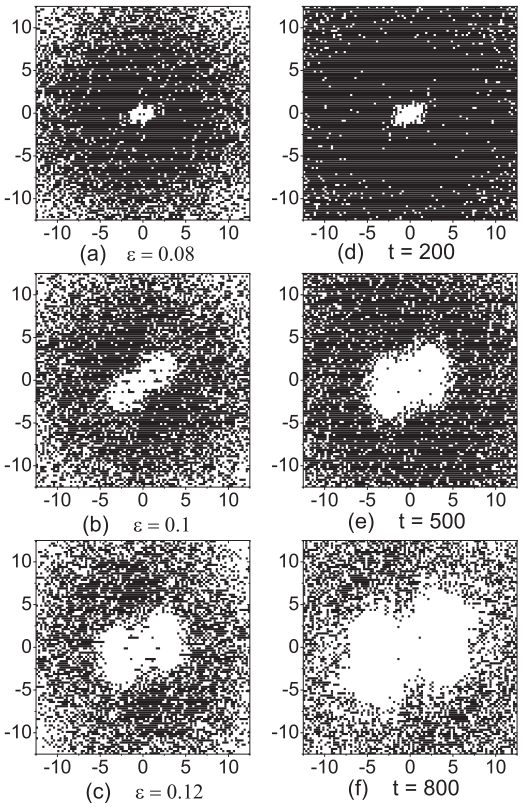

FIG. 3. With the same target that was used in Fig. 1(b), the transition (left column) and transient states (right column) of the pinning regulation shown in the Fourier space. In each subplot, the horizontal and vertical axes represent, respectively, the wave numbers k_x and k_y. (a)–(c) The typical intermediate states appeared in the pinning transition. (d)–(f) For $\varepsilon = 0.2 > \varepsilon_c$, the typical transient states appeared during the course of pinning regulation. The white-colored points correspond to modes that have amplitude smaller than $1 \times 10^{-3}\bar{\phi}_k$, that is, the modes that are stabilized by the pinning, with $\bar{\phi}_k$ the largest mode amplitude of the reference turbulence state.

the given pinning strength and predefined target (the controllable case), we wish to know, at moment t of the pinning, to which degree the turbulence will be regulated. Using the same simulation as for Fig. 1(b), we plot in Fig. 3 (the right column) several of the transient states appearing at different moments of the regulation. It is seen that, similar to the regulation transition, the perturbation modes are also suppressed by the sequence of wave number. More specifically, with the increase of time, the suppressed modes are found to be gradually extended from the center to the periphery. This feature of the transient dynamics can be also inferred from Eq. (7), which shows that, compared to the short-wave modes, the long-wave modes have the faster damping rate.

While having the advantage of regulating turbulence into different spatiotemporal patterns, the pinning method also poses some technical challenges in real applications. Among others, the time delay of the pinning signal and the limited pinning site are two major concerns for the real application of the pinning method. A complete loop of the pinning scheme includes as least three stages: system detection, variable comparison, and signal feedback. To make the pinning method work, a basic requirement is that the time delay caused by the control loop should be smaller than the characteristic time of the system dynamics, which, for our case of drift-wave plasma turbulence, is of the order of 1 ms. Meanwhile, the pinning method in the present work requires inputting feedback signal to each site of the system, that is, the global pinning, which is also hard to be realized in practice. These problems, however, might be solvable by modern engineering technology and the improved control schemes. In particular, with the microelectromechanical-systems (MEMS) technology, now it is possible to reduce the time delay to the millisecond level and, in the meanwhile, arrange a significant number of microsensors (microactuators) in the system to mimic the global pinning. It is worth noting that the drift-wave turbulence studied here can also be regulated by pinning a part of the system sites, that is, the localized pinning. For instance, using $\varepsilon = 1.5$, the regulation shown in Fig. 1(b) can also be accomplished by pinning only 25% of the system sites. (A detail study on the regulation of drift-wave turbulence by the localized pinning will be presented elsewhere [27].)

In summary, we have investigated the regulation of drift-wave turbulence described by a 2D plasma model based on the method of pinning coupling. An explicit formula has been obtained on the relationship between the system controllability and the pattern structure of the target, and verified by numerical simulations. Moreover, in both the transition and transient process of the regulation, it is found that the perturbation modes are suppressed in a hierarchical fashion, that is, by the sequence of wave number. These findings could be helpful to the design of new turbulence-control schemes in real applications, as well as deepening our understanding on the dynamics of drift-wave turbulence.

This work was supported by the National Natural Science Foundation of China under Grant No. 10805038 and by the Chinese Universities Scientific Fund. This work was also supported by the National Basic Research Program of China under Grant No. 2008CB717806 and the China ITER Program under Grant No. 2009GB105005.

[1] *Handbook of Chaos Control*, edited by H. G. Schuster (Wiley-VCH, Weinheim, 1999).
[2] M. Ding, E.-J. Ding, W. L. Ditto, B. Gluckman, V. In, J.-H. Peng, M. L. Spano, and W. Yang, Chaos **7**, 644 (1997).
[3] S. Boccaletti, C. Grebogi, Y.-C. Lai, H. Mancini, and D. Daza, Phys. Rep. **329**, 103 (2000).
[4] G. Hu and Z. Qu, Phys. Rev. Lett. **72**, 68 (1994).
[5] R. O. Grigoriev, M. C. Cross, and H. G. Schuster, Phys. Rev. Lett. **79**, 2795 (1997).
[6] J. Xiao, G. Hu, J. Yang, and J. Gao, Phys. Rev. Lett. **81**, 5552 (1998).
[7] L. Junge and U. Parlitz, Phys. Rev. E **61**, 3736 (2000).
[8] L. Yang, X. Wang, Y. Li, and Z. Sheng, Europhys. Lett. **92**, 48002 (2010).

[9] J. Yang, G. Hu, and J. Xiao, Phys. Rev. Lett. **80**, 496 (1998).
[10] G. Hu and K. He, Phys. Rev. Lett. **71**, 3794 (1993).
[11] Z. Cao, P. Li, H. Zhang, F. Xie, and G. Hu, Chaos **17**, 015107 (2007).
[12] S. Guan, Y. C. Zhou, G. W. Wei, and C.-H. Lai, Chaos **13**, 64 (2003).
[13] S. Guan, G. W. Wei, and C.-H. Lai, Phys. Rev. E **69**, 066214 (2004).
[14] T. Pierre, G. Bonhomme, and A. Atipo, Phys. Rev. Lett. **76**, 2290 (1996).
[15] E. Gravier, X. Caron, G. Bonhomme, and T. Pierre, Phys. Plasmas **6**, 1670 (1999).
[16] T. Klinger, C. Schröder, D. Block, F. Greiner, A. Piel, G. Bonhomme, and V. Naulin, Phys. Plasmas **8**, 1961 (2001).
[17] C. Schröder, T. Klinger, D. Block, A. Piel, G. Bonhomme, and V. Naulin, Phys. Rev. Lett. **86**, 5711 (2001).
[18] G. Tang, K. He, and G. Hu, Phys. Rev. E **73**, 056303 (2006).
[19] F. Brochard, G. Bonhomme, E. Gravier, S. Oldenbürger, and M. Philipp, Phys. Plasmas **13**, 052509 (2006).
[20] A. Pironti and M. L. Walker, Control Syst. Mag. **25**, 30 (2005).
[21] P. H. Diamond, S I. Itoh, K. Itoh, and T. S. Hahm, Plasma Phys. Controlled Fusion **47**, R35 (2005).
[22] K. Pyragas, Phys. Lett. A **170**, 421 (1992).
[23] A. Hasegawa and K. Mima, Phys. Rev. Lett. **39**, 205 (1977).
[24] M. J. Burin, G. R. Tynan, G. Y. Antar, N. A. Crocker, and C. Holland, Phys. Plasmas **12**, 052320 (2005).
[25] S. Y. Yang, Y. C. Zhou, and G. W. Wei, Comput. Phys. Commun. **143**, 113 (2002).
[26] T. Tel and Y.-C. Lai, Phys. Rep. **460**, 245 (2008).
[27] P. Liu, L. Yang, Z. Deng, and X. Wang (preprint).